Low-Temperature Reaction of Buried Metal–Silicon Interfaces: The Evolution of Interfacial Structure

Thomas Novet, John M. McConnell, and David C. Johnson*

Department of Chemistry and Materials Science Institute, University of Oregon, Eugene, Oregon 97403

Received January 16, 1992

Little is known about the initial stages of solid state reactions due, in part, to the lack of suitable experimental probes of buried interfaces. In this paper, the evolution of iron–silicon and titanium–silicon interfaces with temperature and time was investigated by taking advantage of the unique properties of multilayer composites. The structure of the interfaces was monitored by following the changes in the intensities of the Bragg reflections resulting from the superlattice structure. In iron–silicon thin-film multilayer composites, a gradual decrease in diffusion rates and repeat unit size with time, suggest the elimination of unstable configurations with annealing. In titanium–silicon composites, the evolution of the interfaces was much more complex. The repeat unit of the multilayer was found to decrease by 16% during annealing. Even more striking was the development of a compositional plateau at the interface. On the basis of the behavior of these interfaces, a mechanism for the initial stages of a solid-state reaction is presented.

Introduction

Molecular synthesis is dominated by solution-phase reactions, which are typically homogeneous. The nature of these systems has facilitated the use of experimental probes to follow the evolution of the reactions. In these reacting systems, the energy barrier for diffusion is small compared to the energy required for the breaking and re-forming of chemical bonds. Consequently, the rate-limiting steps of these reactions is often the breaking of bonds in the reactants. This has led to the importance of reaction mechanisms, which are used to describe the progress of the reaction and predict product distributions.

Unlike molecular reactions, solid-state reactions occur primarily at the interfaces of heterogeneous systems. Diffusion of the reactants is often the rate-limiting step. Little is known about how these reactions proceed.[1] Without knowledge of a reaction mechanism, it is impossible either to predict or to control a reaction in a rational manner.[2] An experimental technique that gives the ability to monitor the initial stages of the diffusion reaction would aid in the development of reaction mechanisms for solid-state systems.

Due to their small proportion relative to the bulk, interfaces are experimentally difficult to probe.[3] This difficulty is compounded by the fact that the interfaces of most interest to the solid-state chemist are also buried within a material and therefore inaccessible via most surface science techniques. Obtaining more information concerning the development of an interface with time and temperature is vital. Interfaces represent a challenging region of study, one which will be one of the next frontier areas of materials science and chemistry.

Our approach to probing interfacial reactions has been to take advantage of the large density of interfaces which can be found in multilayer composites. These composites are prepared in an ultrahigh vacuum deposition system by sequentially depositing elemental layers of the desired thickness. Thickness can be controlled to create a multilayer modulated on a tens of angstroms length scale. The resulting layers are frequently amorphous as deposited. The very high density of interfaces in these modulated composites permits the thermodynamics of the interfacial reactions to be explored using differential scanning calorimetry.[4] If the repeat thickness of the elemental layers is held constant, the resulting composite behaves like a one-dimensional crystal. The repeating unit of amorphous elemental layers is the unit cell, and the composite diffracts X-rays due to its modulated structure.[5-8]

The resulting diffraction pattern from the superlattice contains much information concerning the structure of the repeat unit. As in conventional single-crystal diffraction studies, the position of the Bragg diffraction peaks permits the repeat distance of the composite to be determined. Since the individual elemental layers are usually amorphous, the intensities of the diffraction peaks cannot be used to determine exact atomic positions as in conventional single crystal crystallography. However, the intensity of the Bragg peaks gives information about the width and shape of the concentration profiles at the interface of the elemental layers.[6,9]

The focus of this paper is the use of variable-temperature X-ray diffraction to probe how buried solid-state interfaces react. As the temperature of a multilayer composite is increased, the interfaces begin to react causing the electron densities of the repeat unit to change. We monitor the resulting changes in the intensities of the multilayer diffraction pattern as a function of time and temperature. The low-temperature solid-state interdiffusion reactions in the iron–silicon and titanium–silicon systems are presented. The results obtained from these two systems are compared and contrasted to demonstrate the influence of chemistry upon the interdiffusion reaction. The ability to use variable-temperature X-ray diffraction to explore the initial stages of a solid-state reaction and give previously unobtainable details of the evolution of

---

(1) Corbett, J. D. In *Synthesis of solid-state materials*; Cheetham, A. K., Day, P., Eds.; Clarendon Press: Oxford, 1987; p 2.
(2) Schäfer, H. *Angew. Chem., Int. Ed. Engl.* 1971, *10*, 43–50.
(3) Weaver, J. H. *Phys. Today*, 1986, *Jan*, 24–30.
(4) Cotts, E. J.; Meng, W. J.; Johnson, W. L. *Phys. Rev. Lett.* 1986, *57*, 2295–2298.
(5) Spiller, E. *Rev. Phys. Appl.* 1988, *23*, 1687–1700.
(6) Bartels, W. J.; Hornstra, J.; Lobeek, D. J. W. *Acta Crystallogr.* 1986, *A42*, 539–545.
(7) Le Boité, M. G.; Traverse, A.; Névot, L.; Pardo, B.; Corno, J. *J. Mater. Res.* 1988, *3*, 1089–1096.
(8) Névot, L.; Croce, P. *Rev. Phys. Appl.* 1980, *15*, 761–779.
(9) Névot, L.; Pardo, B.; Corno, J. *Rev. Phys. Appl.* 1988, *23*, 1675–1686.

0897-4756/92/2804-0473$03.00/0

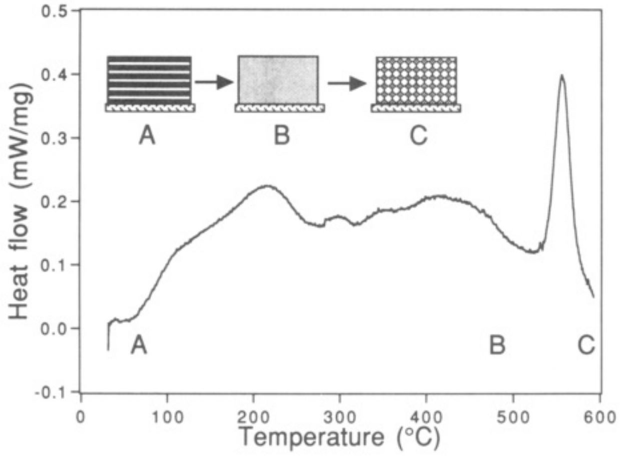

Figure 1. Differential scanning thermograph of the Fe–Si composite showing an initial broad exotherm due to diffusion and a subsequent sharp exotherm due to crystallization.

buried interfaces is stressed.

Experimental Section

Synthesis of Modulated Composites. The amorphous, modulated composites of iron–silicon and titanium–silicon used in this study were prepared in an ultrahigh vacuum deposition system which is described in detail elsewhere.[10] The elements were deposited using electron beam heating controlled by quartz crystal thickness monitors. Deposition rates of 0.5 Å/s were used, and the background pressure during deposition was 5×10^{-8} Torr. X-ray diffraction samples were deposited upon polished (±3 Å rms) silicon wafers. Differential scanning calorimetry samples were deposited upon silicon wafers coated with poly(methyl methacrylate) (PMMA). The iron–silicon sample studied had a composition of 3 iron to 1 silicon. The titanium–silicon samples studied had a stoichiometry of 1 titanium to 1 silicon.

Differential Scanning Calorimetry (DSC). Heat produced by interfacial reactions was quantified using DSC. Approximately 1 mg of freestanding composite was obtained by dissolving the PMMA substrate in acetone and collecting the suspended composite particles via sedimentation into an aluminum DSC pan. The sample was placed in a TA Instruments 910DSC module and heated at 10 °C/min from room temperature to 600 °C under flowing nitrogen. Two background data sets were subsequently collected to obtain an accurate baseline correction. The signal resulting from irreversible interfacial diffusion and crystallization of the composite was obtained by taking the difference between the first run and the subsequent background runs.

Grazing Angle X-ray Diffraction. The X-ray diffraction experiment used a Scintag XDS-2000 θ–θ powder diffractometer in which the original sample holder was replaced by a custom system which has provisions for rapid and reproducible alignment. The design is based upon a pair of optical flats against which the sample is pressed. The height of the optical flats can be adjusted with a vertical micrometer mounting stage. A combined vacuum and sample heating assembly which radiatively heats the sample and stage can be placed around the sample stage.

After the sample stage was aligned at room temperature, the high-temperature shroud was placed about the sample and a vacuum of 5×10^{-7} Torr was obtained. The sample was realigned by maximizing the intensities of the first- and second-order Bragg diffraction peaks via angular and height adjustments. The temperature was then raised to that corresponding to the beginning of the first exotherm on a differential scanning calorimetry trace of the same sample, and alignment was again checked. Diffraction scans were then conducted every 30 min. Maintaining alignment was critical, as small variations in alignment lead to large intensity changes in specular and Bragg reflections. The intensity of the X-ray specular reflectance was monitored to determine if the sample remains stationary during these scans. If the sample shifted during these measurements, the data were discarded.

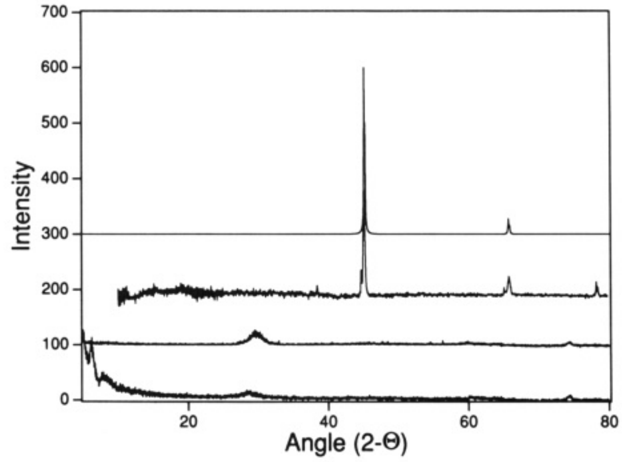

Figure 2. X-ray intensity as a function of 2θ for an as-deposited Fe–Si composite (lowest curve), the same composite annealed at 270 °C and cooled (second curve from bottom), and the sample annealed at 600 °C and cooled (third curve from bottom). The upper curve is calculated using data from the JCPDS diffraction files for Fe_3Si confirming the assignment of the crystallized sample as Fe_3Si.

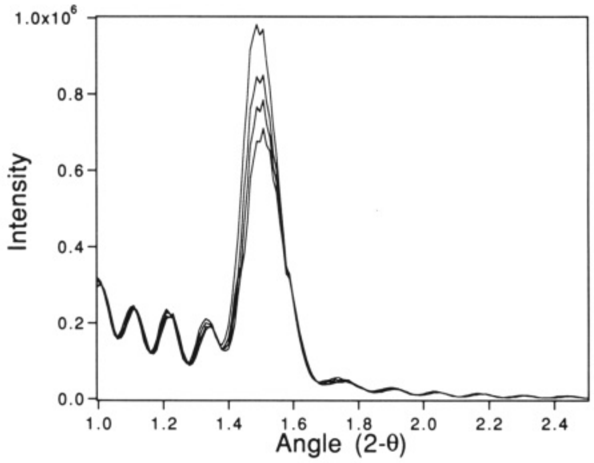

Figure 3. Series of grazing angle X-ray diffraction scans at Fe–Si composite taken as a function of temperature and time illustrating the decay of the diffraction signal intensity without broadening. The peak at 1.5° is the first-order Bragg peak. The smaller peaks arise from the finite number of layers in the sample and their constant intensity implies that the sample maintains coherency during the diffusion process.

Results

The onset and nature of the interfacial reactions in the superlattices of iron–silicon and titanium–silicon were determined by DSC. In all of the samples investigated, an exotherm due to interdiffusion of the composite was clearly separated from the subsequent nucleation of any crystalline compounds. Figure 1 contains a representative DSC trace of the iron–silicon sample. High-angle X-ray diffraction patterns obtained at points A, B, and C (Figure 2) indicate that the first exotherm is due to interdiffusion of the multilayer while the second exotherm is due to crystallization of Fe_3Si. Data from the titanium–silicon samples also contains two distinct exotherms: a broad exotherm from 150–300 °C due to interdiffusion and a sharper exotherm at 550 °C due to crystallization of TiSi. The crystallization temperature of the homogeneous amorphous titanium–silicon alloy agrees well with that determined by Holloway for samples prepared via sput-

---

[10] Fister, L.; Li, X. M.; Novet, T.; McConnell, J.; Johnson, D. C. Manuscript in preparation.

tering.[11] The DSC data combined with the diffraction studies indicate that all of the samples are initially layered and amorphous. The interfaces initially react via an exothermic interdiffusion to produce a homogeneous amorphous alloy which upon subsequent heating exothermically crystallizes.

The multilayer composites were studied via variable-temperature X-ray diffraction. The decay of the superlattice Bragg reflections with time due to interdiffusion of iron and silicon at 150 °C is shown in Figure 3. These data confirm the assignment of the first DSC exotherm to diffusion. Importantly, the width at half-maximum does not increase as the signal decays with time, and the intensity of the subsidiary maxima also does not change with time. These two observations indicate that the interdiffusion at the interfaces is a coherent process; all of the interfaces are diffusing at the same rate.[12]

This interdiffusion of iron and silicon can be analyzed using Fick's laws for diffusion. Fick's laws of diffusion are a phenomenological model originally developed for high temperature diffusion over relatively long distances.[13] Fick's second law of diffusion relates the change in concentration with respect to time to the concentration gradient. The one-dimensional case is given by

$$\frac{\partial c}{\partial t} = \frac{\partial}{\partial x}\left[D \frac{\partial c}{\partial x}\right] \tag{1}$$

where c is the atom fraction of one of the components, x is a spatial coordinate normal to the surface of the composite, t is time, and D is an interdiffusion coefficient. The derivation of this equation assumes a chemical potential gradient across the region of varying composition, and it is assumed that the diffusion medium is a continuum and that higher order terms in the concentration gradient can be neglected. If one also assumes that the interdiffusion coefficient is independent of position (and therefore independent of composition), eq 1 simplifies to

$$\frac{\partial c}{\partial t} = D \frac{\partial^2 c}{\partial x^2} \tag{2}$$

By using the relationship between diffraction intensity and Fourier expansion coefficients of the concentration profile, it is easily shown that the intensity of the superlattice Bragg diffraction peaks should decay according to

$$\frac{\mathrm{d}}{\mathrm{d}t}\left[\ln\left(\frac{I}{I_0}\right)\right] = \frac{-8\pi^2 n^2}{d^2} D \tag{3}$$

where d is the repeat distance of the modulation and n is the order of each of the Bragg reflections.[14] Each Bragg reflection should decay at a rate such that each decay produces the same diffusion coefficient. A plot of ln (I/I_0) versus $-8\pi^2 n^2 t/d^2$ should yield the same straight line for all Bragg reflections, the slope of which is the interdiffusion coefficient.

The intensity data given in Figure 3 for the iron-silicon composite are replotted according to eq 3 in Figure 4. The diffraction data for the two diffraction orders studied fall on the same line, indicating that the simple picture described above is adequate in explaining our initial experimental results. The second-order diffraction peak decays 4 times faster than the first-order diffraction peak as required by eq 3. The slope of these lines give the interdiffusion coefficient for this diffusion couple as 1.3×10^{-19} cm^2/s at 150 °C. In an attempt to determine an activation energy for the interdiffusion process, a subsequent, more complete data set on the same iron-silicon composite was collected.

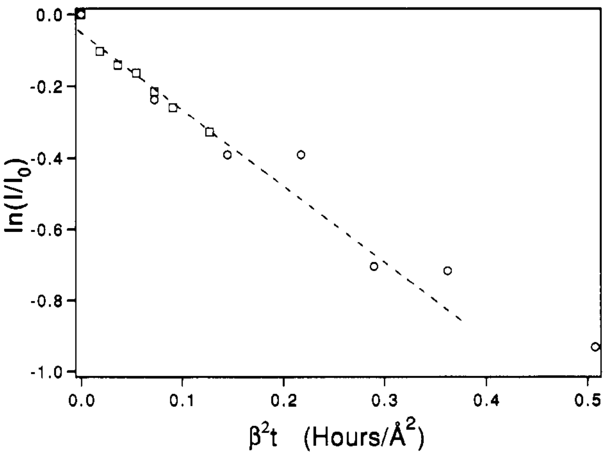

Figure 4. Variation of the intensities of the first- (□) and second order- (○) Bragg peaks in an iron-silicon modulated film annealed at 150 °C. Slope of ln (I/I_0) vs $\beta^2 t$ plot, where $\beta = 2\pi n/d$, yields an interdiffusion coefficient of 1.3×10^{-19}.

Interdiffusion in this second iron-silicon sample was monitored at 100 °C for 12 h followed by 12 h at 110 °C, 12 h at 135 °C and 12 h at 159 °C. These data contain several discrepancies from the simple picture painted above. For the three highest temperatures studied, the second-order Bragg reflection initially decays 4 times faster than the first-order Bragg reflection as we expected from our initial experiment at 150 °C. At 100 °C, however, the second-order Bragg reflection decays more slowly than expected from the decay of the first-order Bragg reflection. This phenomenon will be discussed in more detail later.

The data also deviate from eq 3 at long times for each of the data sets. The diffusion process appears to slow down as the sample is annealed at a particular temperature. Data collected on the original iron-silicon sample at longer times confirmed the slowing of the diffusion process with annealing time. Previous diffraction studies on the decay of metal-metal superlattice reflections as a function of time have also shown an initial fast diffusion process followed by a slower, limiting diffusion rate.[15] It was suggested that the change in the diffusion rate with time might either be due to changes in microstructure or changes in the macroscopic stresses in the superlattice. We believe that the decrease in the diffusion rate is caused by elimination of defects and a corresponding increase in the activation energy for diffusion due to the selective elimination of the most mobile and energetically unfavored conformations. The amorphous modulated composites are internally unstable in that they continuously transform to amorphous states of lower free energy.

The decrease in the number of high-energy conformations and voids with time and temperature is given strong support by the decrease in the repeat unit length with time as shown in Figure 5. The initially deposited composites have a very nonequilibrium distribution of conformations. A high concentration of voids and other unstable confor-

---

(11) Holloway, K. L. Ph.D. Dissertation, Stanford University, 1989.

(12) Falco, C. M. In *Growth of metallic and metal-containing superlattices*; Dhez, P., Weisbuch, C., Eds.; Plenum Press: New York, 1988; pp 3-15.

(13) Greer, A. L.; Spaepen, F. In *Diffusion*; Chang, L. C., Giessen, B. C., Eds.; Academic Press: New York, 1988; pp 419-486.

(14) Murakami, M.; Segmüller, A.; Tu, K. N. In *X-Ray Diffraction Analysis of Diffusion in Thin Films*; Tu, K. N., Rosenberg, R., Eds.; Academic Press: New York, 1988; pp 201-248.

(15) Philophsky, E. M.; Hilliard, J. E. *J. Appl. Phys.* **1969**, *40*, 2198-2205.

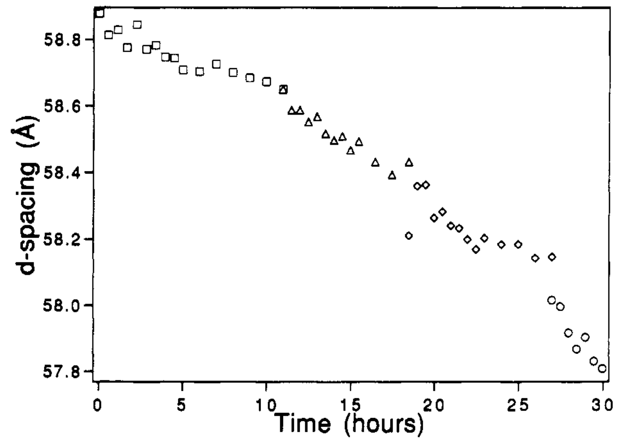

Figure 5. Variation in the position of the first-order Bragg reflection of an iron–silicon modulated film as a function of annealing at 100 °C (□), 110 °C (△), 135 °C (◇), and 159 °C (○). The shift in the position of this reflection is proportional to the decrease in the size of the repeat unit during the interdiffusion of the superlattice.

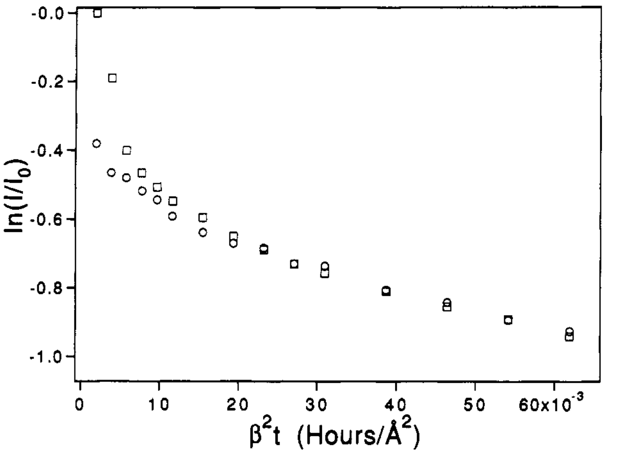

Figure 6. Variation of the intensity of the first order Bragg peak in a titanium–silicon modulated film as deposited and annealed at 271 °C (□) and preannealed at 244 °C then annealed at 271 °C (○).

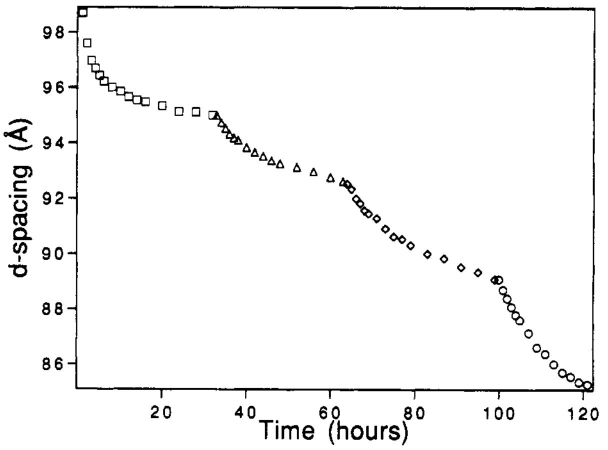

Figure 7. Variation in the thickness of the multilayer spacing as calculated from the position of the first-order Bragg reflection of a titanium–silicon sample. Data were collected while annealing sample at 217 °C (□), 244 °C (△), 271 °C (◇), and 298 °C (○).

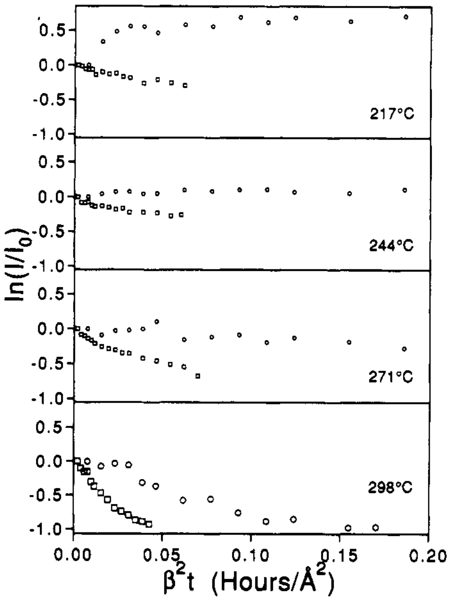

Figure 8. Variation of the intensities of the first- (○) and second-order (□) Bragg peaks in a titanium–silicon modulated film with time when annealed at the indicated temperatures. Data are plotted as ln (I/I_0) vs $\beta^2 t$ to emphasize the deviations from Fick's second law of diffusion.

mations is present in the composite as a result of the quenching of the atoms from the gas phase onto the deposition surface. Diffusion will occur through energetically accessible defects. As the temperature is raised, more high-energy conformations become accessible as diffusion pathways. The concentration of these conformations will decrease with time as the most energetically unfavorable pathways are eliminated.

To confirm that diffusion paths are indeed being eliminated during the annealing process, an as-deposited titanium–silicon sample and one preannealed at 244 °C were heated to 271 °C. Intensities of the first-order Bragg peak as a function of time are shown in Figure 6. The initial diffusion rate is a factor of 5 higher in the sample heated immediately to 271 °C, but the data at longer times are virtually identical to those obtained in the sample which had been annealed at lower temperatures. These data suggest that annealing of the composites selectively eliminates low activation energy diffusion paths.

The data described above suggest the following picture for the evolution of the composite: As the temperature is raised, the composite lowers its total energy through the elimination of high-energy conformations frozen in the composite during deposition and by the lowering of chemical potential due to the mixing of the elements. This diffusion-limited process continues until the initial structural modulation has been completely diffused away. This mixing can account for up to 90% of the total heat of formation of crystalline iron silicide.[16] The last 10% of the heat of formation is released when the amorphous alloy crystallizes.

To expand upon these observations, we investigated a more reactive silicide system. The titanium–silicon system was chosen since titanium and silicon react approximately 4 times more exothermically than iron and silicon.[17] The increased reactivity of titanium–silicon caused several experimental problems including an occasional explosive reaction of the layered composites upon application of mechanical stress. This increased reactivity offered an opportunity to study a system in which chemistry should play a larger role in the interdiffusion reaction.

The titanium–silicon system diffraction data again suggest that diffusion is coherent. The line widths of the

---

(16) Novet, T.; Johnson, D. C. *J. Am. Chem. Soc.* **1991**, *113*, 3398–3403.

(17) Schlesinger, M. E. *Chem. Rev.* **1990**, *90*, 607–627.

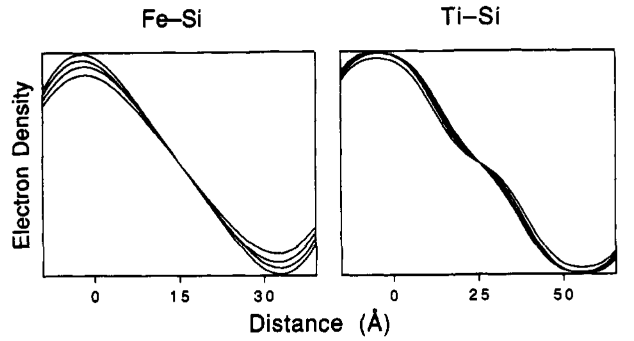

Figure 9. Schematic of the evolution of a Fe–Si and a Ti–Si interface utilizing intensity data presented in this paper and an arbitrary phase relationship illustrating the difference in the behavior of these two interfaces.

Bragg diffraction peaks do not change with time. As with the iron–silicon sample, the size of the repeat unit was found to decrease during annealing. Nearly a 16% change was observed over the course of the experiment (Figure 7). Previous studies involving the reaction of thicker elemental layers also showed a dramatic decrease in the repeat unit size.[11] The cell size decrease results from the increased density of the binary alloy relative to unreacted titanium and silicon layers.

Evidence for dramatic changes in the structure of the composite during the interdiffusion of the elements is found in the changes in the Bragg intensities with time at various temperatures as plotted in Figure 8. The intensities of the second-order Bragg reflections actually increase during the lower temperature anneals! The growth of this Bragg reflection results from developing structure or asymmetry of the evolving interface. This implies that the interdiffusion coefficient is not independent of composition.[18] The compositional dependence on the diffusion constant is chemically reasonable given the large variation in formation enthalpies in titanium silicides.[19] Amorphous alloys of different composition will also have different formation energies. At low temperatures, the free energy is dominated by ΔH, so large differences in ΔH relative to $T\Delta S$ can lead to the growth of a plateau in composition.

Previous diffraction studies of superlattices have used the measured intensities of the Bragg diffraction peaks to produce an electron density profile of the interfacial region. To create these profiles, it is necessary to assign phase information to the intensity data, and it is typically assumed that the interfaces are atomically abrupt and that the structures are centrosymmetric. Figure 9 contains the changes of the electron density with distance upon annealing for both the iron–silicon and titanium–silicon superlattices making these same assumptions. This figure serves qualitatively to illustrate the evolution of the metal–silicon interface.

Discussion

Studies directed at observing the initial evolution of solid–solid interfaces have been limited to length scales above 20 Å due to the lack of a suitable probe. Sputter depth profiling Auger electron spectroscopy[20] and Rutherford backscattering[21,22] have been useful in monitoring interfaces on longer length scales, but they can yield little information regarding the initial reaction of two solid reactants. The decay of superlattice reflections as a result of interdiffusion is the most sensitive method available to probe for the formation of interfacial structure at reacting interfaces.[13]

Our observations concerning the development of interfacial structure at an amorphous interface of reacting elements gives important insight to the mechanism of both thin-film and bulk reactions. In the 1970s and early 1980s several research groups began to explore the reaction kinetics of thin-film diffusion couples.[23-25] These groups focused their studies on metal–silicon systems. Crystalline films of approximately 500 Å of each element were deposited and subsequently annealed at temperatures of several hundred degrees Celsius. These thin-film diffusion couples were found to be nucleation-limited rather than diffusion-limited systems. A sequential evolution of the various compounds in the phase diagram was observed. The same sequence of phases was observed regardless of the overall composition of the diffusion couple.[26]

Walser and Benê compiled available data on the binary silicides and empirically correlated the first phase formed in a thin-film diffusion couple with information contained in bulk equilibrium phase diagrams.[27] Their "first phase rule" states "The first compound nucleated in planar binary reaction couples is the most stable congruently melting compound adjacent to the lowest temperature eutectic on the bulk equilibrium phase diagram." This empirical rule is remarkably successful at predicting the first phase formed in thin-film diffusion couples.

Walser and Benê speculated that the physical basis for their rule was related to the composition of an amorphous region which they suggested develops at the interface between two solid reactants. Our data support the formation of an amorphous region at the interface between reacting elements. We are able to observe the formation of a composition plateau in the titanium silicon system. We believe that this plateau is the precursor to the formation of a crystalline compound.

Initial reactions in bulk solids should follow the same path as the reaction in the thin-film multilayer. With increasing temperature and time, an amorphous interfacial region will grow in spatial extent, decreasing the concentration gradients. The decreased concentration gradients will decrease the diffusion rates and added structure is likely to develop due to differences in diffusion rates with composition. This added structure or compositional plateaus are the most likely sites for the nucleation of crystalline compounds. As the thickness of the interfacial compound grows with time, this process will repeat itself at the new interfaces.

Summary

Analysis of diffraction data from amorphous superlattice composites permits a detailed picture of the earliest stages of the solid-state reaction of titanium and iron with silicon to be visualized. The initial stage of this reaction is the interdiffusion of the elements to form an amorphous interfacial region which contains the concentration gradient

---

(18) Fleming, R. M.; McWhan, D. B.; Gossard, A. C.; Wiegmann, W.; Logan, R. A. *J. Appl. Phys.* **1980**, *51*, 357–363.

(19) de Boer, F. R.; Boom, R.; Miedema, A. R. *Physica B* **1980**, *101B*, 294–319.

(20) Raaijmakers, I. J. M. M.; Reader, A. H.; Oosting, P. H. *J. Appl. Phys.* **1988**, *63*, 2790–2795.

(21) Brasen, D.; Willens, R. H.; Nakahara, S.; Boone, T. *J. Appl. Phys.* **1986**, *60*, 3527–3531.

(22) Holloway, K.; Sinclair, R. *J. Appl. Phys.* **1987**, *61*, 1359–1364.

(23) Herd, S.; Tu, K. N.; Ahn, K. Y. *Appl. Phys. Lett.* **1983**, *42*, 597.

(24) Gas, P.; d'Heurle, F. M.; Goues, F. K.; La Placa, S. J. *J. Appl. Phys.* **1986**, *59*, 3458–3466.

(25) Canali, C.; Cetellani, F.; Ottaviani, G.; Celotti, G. *Appl. Phys. Lett.* **1978**, *50*, 255–258.

(26) Tsaur, B. Y.; Lau, S. S.; Mayer, J. W.; Nicolet, M.-A. *Appl. Phys. Lett.* **1981**, *38*, 922–924.

(27) Walser, R. M.; Benê, R. W. *Appl. Phys. Lett.* **1976**, *28*, 624–625.

between the elements. At low temperatures and short diffusion distances, this region may contain added structure due to the formation of particularly stable amorphous alloy compositions. In iron–silicon, this region develops in a smooth manner without any significant added structure. In titanium–silicon, a significant plateau of a particular composition of amorphous alloy is found to develop.

Acknowledgment. We acknowledge the assistance of L. Fister, Bernard Wendring, and C. Grant for helpful discussions and advice while developing the experimental procedures used in this paper. This work was supported by a Young Investigator Award from the Office of Naval Research (N00014-87-K-0543). Support by the National Science Foundation (DMR-8704652), the donors of the Petroleum Research Fund, administered by the American Chemical Society, and the University of Oregon is also gratefully acknowledged.

Registry No. Si, 7440-21-3; Fe, 7439-89-6; Ti, 7440-32-6.

Structure and Chemistry of Silicon Nitride and Silicon Carbonitride Thin Films Deposited from Ethylsilazane in Ammonia or Hydrogen

Y. W. Bae, H. Du, and B. Gallois

Department of Materials Science and Engineering, Stevens Institute of Technology, Hoboken, New Jersey 07030

K. E. Gonsalves†

Department of Chemistry and Chemical Engineering, Stevens Institute of Technology, Hoboken, New Jersey 07030

B. J. Wilkens

Bellcore, Red Bank, New Jersey 07701

Received August 12, 1991. Revised Manuscript Received February 24, 1992

Amorphous silicon nitride or silicon carbonitride thin films were deposited on (100) silicon substrates by the pyrolysis of ethylsilazane, $[CH_2CH_3SiHNH]_n$, in ammonia or hydrogen in the temperature range 873–1073 K at 0.1 MPa. Studies by means of Auger electron spectroscopy, Rutherford backscattering spectroscopy, and nuclear reaction analysis indicated the removal of carbon species present in the precursor to yield silicon nitride when the deposition was carried out in ammonia. Carbon-related bonds were, however, partially ruptured in the precursor when hydrogen was used, resulting in the formation of silicon carbonitride. The hydrogen content was determined by elastic recoil detection to decrease from 18 to 10 ± 1% in silicon nitride and from 21 to 8 ± 1% in silicon carbonitride with increasing deposition temperature. Fourier transform infrared spectroscopy analysis showed only Si–H_n bonds ($n = 1, 2, 3$) in silicon carbonitride and only N–H_n bonds ($n = 1, 2$) in silicon nitride. The refractive index increased with the deposition temperature from 1.86 to 2.10 for silicon nitride and from 1.81 to 2.09 for silicon carbonitride. The average deposition rate measured by ellipsometry increased with temperature from 1.9 to 49 nm/min. The apparent activation energies calculated from the slopes of the Arrhenius plot were equal to 19 and 43 kJ/mol in the mass transport regime and to 181 and 197 kJ/mol in the kinetic regime for silicon carbonitride and silicon nitride, respectively.

Introduction

As a consequence of their superior physical, chemical, and thermal properties, silicon nitride and silicon carbonitride thin films have been the subject of extensive research during the past two decades for both structural and microelectronic device applications. Chemical vapor deposition (CVD) is commonly used to produce thin films of these materials.[1] Many different chemical species have been used to form silicon nitride, but most involve reactions between silane[2-4] or a silicon halide[1,5] and either ammonia or nitrogen in the temperature range 1000–1400 K. Silicon carbonitride has been deposited by adding propane as a carbon source to the gas mixture of silicon halide, ammonia, and hydrogen at temperatures above 1400 K.[6]

Even though CVD provides a unique way to produce both silicon nitride and silicon carbonitride films of high density and purity, irrespective of the substrate geometry,[1] high deposition temperatures have remained a major limitation of this process. High deposition temperatures may lead to interlayer atomic diffusion and thus substrate degradation, to peeling of the film because of mismatch in thermal expansion coefficients, and to temperature-induced changes in the shape or the crystallinity of the substrate.[7] These problems can be minimized, however,

---

† Current address: Institute of Materials Research, University of Connecticut, Storrs, CT 06268.

(1) Niihara, K.; Hirai, T. *J. Mater. Sci.* **1976**, *11*, 593.
(2) Taft, E. A. *J. Electrochem. Soc.* **1971**, *118*, 1341.
(3) Lin, S. S. *J. Electrochem. Soc.* **1977**, *124*, 1945.
(4) Popova, L. I.; Vitanov, P. K.; Antov, B. Z. *J. Non-Cryst. Solids.* **1979**, *31*, 429.
(5) Gebhardt, J. J.; Tanzilli, R. A.; Harris, T. A. *J. Electrochem. Soc.* **1976**, *123*, 1578.
(6) Hirai, T.; Goto, T. *J. Mater. Sci.* **1981**, *16*, 17.

0897-4756/92/2804-0478$03.00/0